FLOMEKO2019
18th International Flow Measurement Conference
Portugal | Lisbon | LNEC | 26-28 june 2019

Identification of coherent structures in horizontal slug flow

M. Olbrich[1,2], E. Schmeyer[1], M. Bär[1], M. Sieber[2], K. Oberleithner[2] and S. Schmelter[1]

[1] *Physikalisch-Technische Bundesanstalt (PTB), Abbestr. 2–12, 10587 Berlin, Germany.*
[2] *Institute of Fluid Dynamics and Technical Acoustics, Technische Universität Berlin, Müller-Breslau-Straße 8, 10623 Berlin, Germany.*
E-mail (corresponding author): marc.olbrich@ptb.de

Abstract

Multiphase flow measurement devices are significantly affected by the occurring flow pattern, such as, e.g., slug flow, leading to large uncertainties. In this context, the slug flow pattern in horizontal pipes is investigated with the aim of finding a statistical characterization of the structures in space and time. For this, two different instances of slug flow are analyzed with a snapshot proper orthogonal decomposition and an additional mode coupling algorithm, which provides an energy-ranked mode basis of the underlying coherent structures. For the considered flows, the most energetic mode pair has been identified with the corresponding slugging structures. Thereby, the temporal and spatial information of these mode pairs enables a statistical characterization of the slugs. In this context, a length scale, a dominant frequency, and an energy representation of the slugging structures is obtained from this method.

1. Introduction

One central aim in multiphase flow metrology is to evaluate and reduce the large uncertainty in multiphase flow metering that reaches up to 20% in the oil and gas industries [11]. For this, the flow pattern in horizontal pipes is of special interest since multiphase flow measurement devices can significantly be affected by liquid slugs and the induced pressure fluctuations and vibrations. Therefore, the process of flow pattern formation is investigated.

In this contribution, we focus on the analysis of horizontal slug flow by means of snapshot proper orthogonal decomposition (snapshot POD), see, e.g., [1,2,4], with an additional mode coupling algorithm, as proposed in [4]. The snapshot POD extracts an energy-ranked mode basis of the coherent structures from the flow data with the aim of representing the relevant flow phenomena (e.g., slugs) by a few elements of the mode basis. This method is applied to spatially and temporally resolved data.

At first, we analyze data obtained from the CFD simulation of an air-water slug flow test case, for which the slugs occur at a fixed frequency of $1\ \mathrm{Hz}$ [6]. Furthermore, the snapshot POD analysis is applied to data from experimental video observations of a nitrogen - brine water slug flow.

Since the flow pattern is characterized by the distribution of the different phases in the pipe, time-resolved phase volume fraction fields from CFD, as well as gray intensity fields from video observations are used for this analysis.
In both slug flows, the most energetic mode pair from snapshot POD provides a statistical characterization of the slugging structures through their temporal and spatial information.

2. Data analysis methodology

2.1 Snapshot proper orthogonal decomposition

The snapshot proper orthogonal decomposition (snapshot POD) is a modal decomposition and often used for the identification and characterization of coherent structures in turbulent flows, see, e.g., [1,2,3,4,5].
For the analysis of coherent structures in the slug flow regime, the snapshot POD is applied to spatially and temporally resolved data of this flow pattern. For this, let $g(x,y,t)$ be a snapshot

sequence of a two-dimensional scalar field. Then, the data is decomposed as follows

$$g(x,y,t) = \overline{g}(x,y) + g'(x,y,t) = \overline{g}(x,y) + \sum_i a_i(t)\,\phi_i(x,y), \quad (1)$$

where $\overline{g}$ denotes the time-averaged data field, g' the corresponding fluctuations, a_i the temporal coefficients and ϕ_i the spatial modes. Furthermore, a_i and ϕ_i can be obtained from an eigenvalue decomposition of the correlation matrix of the fluctuations g' as follows. Let $G \in \mathbb{R}^{M\times N}$ be the matrix of the rearranged fluctuations of the snapshot sequence g' with M rows and N columns, where M denotes the number of spatial points and N denotes the number of snapshots. Here, all spatial points of the i-th snapshot are arranged in the i-th column of G. Then a_i and ϕ_i are obtained from the eigenvalue decomposition of $R := \frac{1}{N} G^T G$:

$$R\,v_i = \lambda_i v_i,\ i = 1,\dots,N, \text{with } \lambda_1 \geq \cdots \geq \lambda_N \geq 0\,. \quad (2)$$

Here, the temporal coefficient a_i is given by the scaled eigenvector v_i with respect to the eigenvalue λ_i as,

$$a_i(t) := \sqrt{N\,\lambda_i}\,v_i \quad (3)$$

and the spatial mode ϕ_i is given as

$$\phi_i(x,y) := \frac{1}{N\lambda_i}\sum_{k=1}^{N} a_i(t_k)\,g'(x,y,t_k) \quad (4)$$

for $i = 1,\dots,N$. In the context of fluid dynamics, a temporal coefficient $a_i(t)$ (Equation (3)) can be interpreted as the dynamical behaviour of an underlying coherent structure of the flow field. The corresponding eigenvalue provides a measure of the energy of this coherent structure. The spatial mode $\phi_i(x,y)$ (Equation (4)) can then be understood as a weighted time-average of the considered flow field fluctuations, weighted with the corresponding dynamics and energy. This provides spatial information of the underlying coherent structure. Further details can be found in [1,2,3,4].

2.2 Mode-coupling algorithm

Since the dynamics of periodic structures can be described by a pair of modes, the mode-coupling algorithm proposed in [4] is used in addition. Related modes are identified by the spectral similarity of their temporal coefficients, which accounts for modes that are shifted by a quarter period. The mode coupling is computed by an additional eigenvalue decomposition

$$Ac_i = \mu_i c_i \quad (5)$$

with $A := \begin{bmatrix} a_1^2 & \cdots & a_N^2 \\ \vdots & \ddots & \vdots \\ a_1^N & \cdots & a_N^N \end{bmatrix}^T \cdot \left(\begin{bmatrix} a_1^1 & \cdots & a_N^1 \\ \vdots & \ddots & \vdots \\ a_1^{N-1} & \cdots & a_N^{N-1} \end{bmatrix}^T \right)^+$,

where a_i^k denotes k-th entry of i-th temporal coefficient a_i and $(\cdot)^+$ denotes the Moore-Penrose pseudo inverse of the corresponding matrix. Note that this is a dynamic mode decomposition (DMD) on the temporal coefficients. The similarity measure of the temporal coefficients a_i and a_j is given by

$$H_{i,j} := \mathrm{Im}\left(\sum_{k=1}^{N} c_k^i\ \overline{c_k^j}\ \mathrm{sgn}\big(\mathrm{Im}(\mu_k)\big) \right), \quad (6)$$

where $\overline{c_k^j}$ denotes the complex conjugate of c_k^j, Im the imaginary part and sgn the sign function. The matrix H is also called *harmonic correlation matrix.* The indices of the coupled modes are then given by the indices of the maximal entries of H, since it indicates the temporal coefficients with the highest spectral similarity. The dominant frequency f of an identified mode pair (a_i, a_j) (equivalently denoted by (ϕ_i, ϕ_j)) is then derived from the corresponding eigenvalue μ_k (Equation (5)) by

$$f = \frac{\mathrm{Im}(\ln(\mu_k))}{2\pi}. \quad (7)$$

To determine the combined energy content of the mode pair (a_i, a_j) the corresponding eigenvalues of the modal decomposition (see Equation (2)) are summarized as

$$E = \frac{\lambda_i + \lambda_j}{\sum_{l=1}^{N}\lambda_l}. \quad (8)$$

Note that E represents the energy distribution in terms of a discrete time signal. It can only be identified with a physical energy if g has appropriate physical units. For details see [4].

3. Data of horizontal slug flow

For the analysis of horizontal slug flow with snapshot POD, two different types of slug flow data are considered.

At first, phase volume fraction fields, obtained from the CFD simulation of a periodic air-water slug flow, are used. Because of its periodicity, this flow is suitable for testing the applicability of snapshot POD.

Second, the method is applied to video observations of an experimental nitrogen-brine water slug flow.

3.1 CFD simulation of periodic air-water slug flow

The simulation of an air-water slug flow through a horizontal pipe with an inner diameter of $D = 0.054\ \mathrm{m}$ and a length of $L = 8\ \mathrm{m}$, was adopted from [6]. The fluid properties and superficial velocities of this flow are given in Table 1.

Table 1: Fluid properties and superficial vel. for CFD.

	water	air
density in $\frac{\mathrm{kg}}{\mathrm{m}^3}$	998.2	1.225
dyn. viscosity in $\mathrm{Pa \cdot s}$	$1.003 \cdot 10^{-3}$	$1.789 \cdot 10^{-5}$
superficial vel. in $\frac{\mathrm{m}}{\mathrm{s}}$	1.0	1.0

For the computation, the pipe was discretized as an O-grid consisting of about 1.1 million nodes (45 nodes in radial, 104 nodes in angular, and 685 nodes in longitudinal direction).

To generate a periodic formation of slugs in the pipe, a time-dependent sinusoidal displacement of the vertical position of the air-water interface is applied to this flow as introduced in [6]. For this, the inlet is initialized with equally distributed phases in the inlet cross section, such that the lower half of the cross section is filled with water and the upper half is filled with air (see Figure 1). The initial condition is obtained from the vertical position of the interface $\tilde{y}_{int}$ by

$$\tilde{y}_{int}(x, t = 0) = \frac{D}{4} \sin\left(2\pi \frac{4x}{L}\right) + \frac{D}{2}, \qquad (9)$$

where t denotes the time and x the spatial component in flow direction (see Figure 1). The time-dependent vertical position of the interface at the inlet is then given by

$$\tilde{y}_{int}(x = 0, t) = \frac{D}{4} \sin\left(2\pi \frac{v\, 4t}{L}\right) + \frac{D}{2}, \qquad (10)$$

where $v = 2\frac{\mathrm{m}}{\mathrm{s}}$ denotes the inlet gas or liquid velocity. This perturbation leads to a periodical slug formation in the pipe of $1\ \mathrm{Hz}$ (see Figure 2).

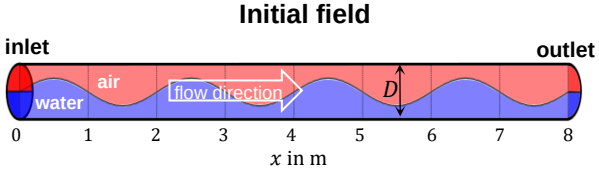

Figure 1: Illustration of the initial field (not to scale).

Furthermore, a no-slip boundary condition at the walls of the pipe and a pressure outlet boundary condition was set.

The CFD simulation was performed in ANSYS FLUENT [10]. For this, an unsteady Reynolds-averaged Navier-Stokes (URANS) approach with the k-ω-SST turbulence model was chosen [8].

To model the gas-liquid interface the volume of fluid (VOF) method was applied within a mixture model [12]. In addition, turbulence damping was included to model such flows with high velocity gradients at the interface correctly [10]. The space and time discretization schemes are chosen as in [12].

In Figure 2, a snapshot of the gas volume fraction field $\alpha_{air}(x, y, t)$ from a longitudinal section of the pipe at $t = 70.86\ s$ is depicted. Here, the time-dependent interface displacement at the inlet is visible along the first meters of the pipe. Further downstream the water slugs are formed.

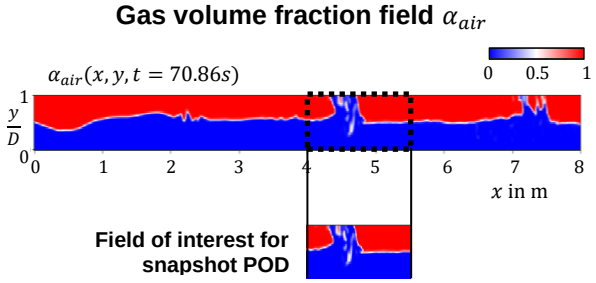

Figure 2: Snapshot of gas volume fraction field from a longitudinal pipe section at $t = 70.86\ s$ with exposed field of interest (not to scale).

To analyze the fully developed slug flow from the simulations with snapshot POD, the gas volume fraction field data is collected from a longitudinal section of a $1.5\ \mathrm{m}$ long pipe segment at $4 - 5.5\ \mathrm{m}$ (see Figure 2). To ensure that numerical effects from the initialization do not affect the flow field anymore and the simulated flow is well developed, the snapshot sequence is collected in a time interval of $10\ s$ from $70\ s$ to $80\ s$ with a sample rate of $100\ \mathrm{Hz}$ (see Figure 3).

3.2 Experimental slug flow

The considered experiment of a horizontal gas-liquid slug flow was performed by TUV SUD NEL. The experimental setup consists of a straight horizontal pipe with an inner diameter of $D = 0.0972\ \mathrm{m}$ and a length of $100\ D$, followed by a Perspex viewing section with a length of $0.5\ \mathrm{m}$, where the slug flow was recorded from aside by a high-speed camera with a frame rate of $240\ \mathrm{fps}$. This section is followed by a right bend and a vertical measurement configuration [11], but this is of minor interest, since the slugging structures in the

horizontal pipe are investigated. The fluid properties and superficial velocities are listed in Table 2.

Table 2: Fluid properties and superficial vel. for experiment.

	Brine water	nitrogen
density in $\frac{\text{kg}}{\text{m}^3}$	1011	10.8
dyn. viscosity in Pa · s	$8.82 \cdot 10^{-4}$	$1.75 \cdot 10^{-5}$
superficial vel. in $\frac{\text{m}}{\text{s}}$	0.545	1.635

To obtain a scalar field representation of the multidimensional RGB-frames from the video, the grayscale is extracted. A snapshot sequence of this grayscale frames for a time interval of $50\,s$ is then used for the analysis with snapshot POD (see Figure 3).

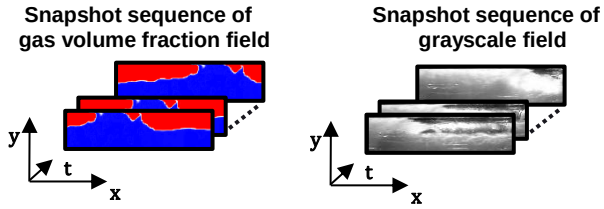

Figure 3: Illustration of snapshot sequences from CFD data (left) and grayscale frames of experimental videos (right).

4. Results

In this chapter, the results of the snapshot POD analysis of the flow field data from CFD and experimental video observations are presented. Since this work focuses on a statistical characterization of the slugging structures, only the relevant results are selected. For both data sets, the coherent structures, represented by the most energetic mode pair can be identified with the slugging structures of the corresponding slug flow. Hence, this mode pair provides spatial and temporal parameters for a characterization of the slugging structures.

4.1 Results for CFD data

In Figure 4, the most energetic mode pair of the air-water slug flow from CFD, as well as the corresponding temporal coefficients and the time-averaged gas volume fraction field are depicted as result of the analysis with snapshot POD. In addition, the vertical position of the gas-liquid interface (liquid level) over time and the averaged slugging structure are also given for validation. The liquid level was extracted from the snapshot sequence at $x = 15D$ with the method of tracking the gas-liquid interface described in [13]. The averaged slugging structure was obtained from the mean of all snapshots with a slug (at centered position).

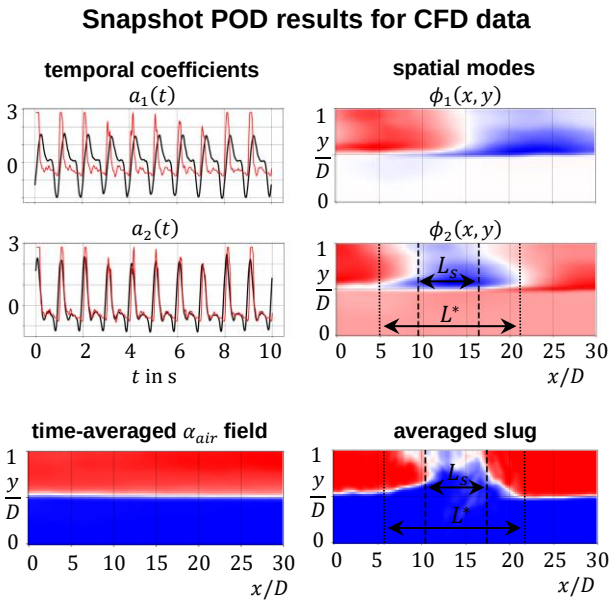

Figure 4: Most energetic mode pair $(\boldsymbol{\phi_1}, \boldsymbol{\phi_2})$ with corresponding temporal coefficients $\boldsymbol{a_1}, \boldsymbol{a_2}$ (—) from snapshot POD in comparison with liquid level over time (—), the averaged slug and the time-averaged gas volume fraction field $\overline{\boldsymbol{\alpha}}_{\boldsymbol{air}}$, obtained from CFD data. In addition, the derived length scales $\boldsymbol{L_s}, \boldsymbol{L^*}$ are given. Note that $\boldsymbol{a_1}, \boldsymbol{a_2}$ and the liquid level are depicted in standard score, respectively. Drawings not to scale.

This mode pair is identified with the averaged slugging structure of the corresponding air-water slug flow, since the temporal coefficients coincides with the liquid level, especially in width and periodicity of the peaks. Note that a_1 is shifted to a_2 as stated in Chapter 2. Furthermore, the frequency of the coupled mode pair (ϕ_1, ϕ_2) of $1\,\text{Hz}$ (see Equation (8)) is equal to the frequency of slug occurrence of the periodic slug flow. The structure displayed in the spatial mode $\phi_2(x, y)$ is interpreted as the averaged slugging structure. This can be verified by the averaged slug, which is also depicted in Figure 4. From that, the slug body length L_s can be derived [14, 15, 16]. This length scale and the slug frequency f provide parameters for a statistical characterization of the slug flow.

Furthermore, an additional length scale L^* can be obtained as proposed in [15]. For this the transitional velocity of a slug v_s is multiplied with the time interval of a slug Δt_s passing by at one point, i.e.:

$$L^* = v_s \cdot \Delta t_s. \tag{11}$$

Based on the unit cell model [14] and the considered specific rectangular shape of a slug, this length scale is often used for the calculation of the slug body length, see [15]. But for slugs, which deviate much in their shape from the unit cell model, this identification is not obvious. Since on strongly tilted

slugging structures as in Figure 4, it is not clear to determine a unique time of a slug front and a slug tail. Nevertheless, the length scale L^* can be obtained from the liquid level over time or rather the temporal coefficient a_2 under knowledge of v_s, since it depends only on temporal information and a velocity. Therefore, a complete peak in between two local minima of the liquid level over time is considered as one slug. Then, the obtained length scale L^* provides an information of the length of the complete structure, and not just the inner part of the slug body. To determine L^*, average parameters are considered, since a statistical characterization is sought. For this, the averaged translational velocity of the slugs is obtained by a cross correlation of a column of the dataset at $x_1 = 0D$ and $x_2 = 30D$ over time. Since the distance is known, the average velocity of the slugs is then derived by the shift of the data obtained by the (unique) maximum of the cross-correlation function. This procedure is adopted from the PIV-measurement technique, see, e.g., [17]. This leads to an average translational velocity $\bar{v}_s = 2.63 \frac{m}{s}$ of the slugging structures.

Since the temporal coefficient a_2 represents the dynamics of the liquid level, the time interval of a slug Δt_s can be approximated by the width of the associated peak from zero to zero. Taking the mean of all these intervals, the average time interval $\overline{\Delta t_s} = 0.31\ s$ can be derived. This results in a length scale for the averaged slugging structure of about $L^* = 16\ D$ which also matches the length of the

Table 3: Parameters for statistical characterization of air-water slug flow from CFD data.

Coupled energy content E of mode pair (ϕ_1, ϕ_2) (see Equation (8))	46.6 %
Frequency f of mode pair (ϕ_1, ϕ_2) (see Equation (7)) (Identified with slugging frequency)	1 Hz
Averaged slug body length L_s	7 D
Averaged structure length L^*	16 D

average slugging structure shown in ϕ_2 and the averaged slug (see Figure 4). The parameters for a statistical characterization of the slugs obtained from analysis with snapshot POD are summarized in Table 3.

4.2 Results for experimental data

In Figure 5, the most energetic mode pair of the experimental nitrogen - brine water slug flow, as well as the corresponding temporal coefficients are depicted as result of the analysis with snapshot POD. Analogously to Figure 4, the liquid level over time, obtained from the experimental video observations with the same method as mentioned in Section 4.1, see [13], is plotted for comparison. Since a snapshot sequence of grayscale fields are analyzed, the modal decomposition accounts for the changes in the gray intensities. For the considered flow, the brine water shows higher gray intensities then the transparent nitrogen in front of the dark background. But the highest gray intensities appear at the gas-liquid interface, due to reflection at the liquid surface. Hence, the spatial modes show coherent structures of the flow in terms of gray intensities, but with a highlighted gas-liquid interface.

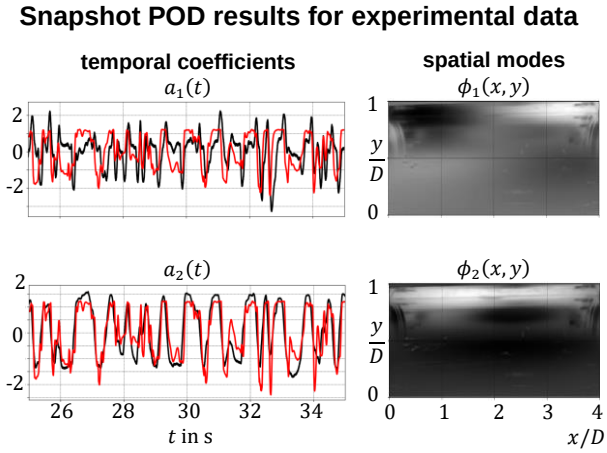

Figure 5: Most energetic mode pair ($\boldsymbol{\phi_1, \phi_2}$) with corresponding temporal coefficients $\boldsymbol{a_1, a_2}$ (—) from snapshot POD in comparison with liquid level over time (—). Note that $\boldsymbol{a_1, a_2}$ and the liquid level are depicted in standard score for a **10 s** time interval [**25 s, 35 s**], respectively. Drawing of $\boldsymbol{\phi_1, \phi_2}$ not to scale.

The depicted mode pair (see Figure 5) is also identified with the averaged slugging structure because of the clear similarity of the liquid level with the corresponding temporal coefficients and the shape of the spatial modes. Since the gas-liquid interface in ϕ_2 occupies the complete length of the field of view, it can be deduced, that the average slug is at least as long as the field of view. Therefore, an average slug body length scale L_s cannot be derived from the spatial mode. Nevertheless, the length scale $L^* = 7.6$ D can be derived from the temporal coefficient a_2. For this, the averaged translational velocity $\bar{v}_s = 2.85 \frac{m}{s}$ and the averaged time interval $\overline{\Delta t_s} = 0.26\ s$ are obtained as explained before in Section 4.1. Furthermore, the dominant frequency f and the energy content E of the selected mode pair is also provided by snapshot POD analysis. These parameters can be used for a statistical characterization of the slugging structures and are summarized in Table 4. Note that the dominant frequency $f = 1.4$ Hz agrees with the averaged frequency of slug occurrence, where the

number of counted slugs (72) is divided by the length of the considered time interval (50 s).

Table 4: Parameters for statistical characterization of nitrogen – brine water slug flow from experimental data.

Coupled energy content E of mode pair (ϕ_1, ϕ_2) (see Equation (8))	55.9 %
Frequency f of mode pair (ϕ_1, ϕ_2) (see Equation (7)) (Identified with slugging frequency)	1.4 Hz
Averaged structure length L^*	7.6 D

4. Conclusion

To characterize the structures of two different slug flows statistically, an analysis with snapshot POD was performed and validated. For both examples, the most energetic mode pair was identified with the slugging structures and used for their characterization in space and time. Altogether, the snapshot POD with an additional mode coupling algorithm is a valid tool for the identification of coherent structures in horizontal slug flow and enables a quantitative characterization of the occurring liquid slugs by their temporal and spatial information.

Acknowledgements
This work was supported through the Joint Research Project "Multiphase flow reference metrology". This project has received funding from the EMPIR programme co-financed by the Participating States and from the European Union's Horizon 2020 research and innovation programme. The authors would like to thank Terri Leonard and Marc MacDonald from TUV SUD NEL, who provided the experimental video observations.

References

[1] Taira K, Brunton S L, Dawson S T M, Rowley C W, Colonius T, McKeon B J, Schmidt O T, Gordeyev S, Theofilis V and Ukeiley L S. "Modal Analysis of Fluid Flows: An Overview", *AIAA Journal*, **Vol. 55**, pp. 4013-4041, 2017.

[2] Holmes P, Lumley J L, Berkooz G. *Turbulence, coherent structures, dynamical systems and symmetrie.* Cambridge University Press, 1996.

[3] Sirovich L, "Turbulence and the dynamics of coherent structures. Part I: Coherent structures", *Quart. Appl. Math.*, **Vol. 45**, pp. 561-571.1987.

[4] Sieber M, Paschereit C, Oberleithner K. "Spectral proper orthogonal decomposition". *Journal of Fluid Mechanics*, **Vol. 792**, pp. 798-828, 2016.

[5] Polanski J, Wang M. "Proper orthogonal decomposition as a technique for identifying two-phase flow pattern based on electrical impedance tomography", *Flow Measurement and Instrumentation*, **Vol. 53**, pp. 126-132, 2016.

[6] Frank T, "Numerical simulation of slug flow regime for an air-water two phase flow in horizontal pipes", in: *The 11th International Topical Meeting on Nuclear Reactor Thermal-Hydraulics (NURETH-11)*, Avignon, France.

[7] Fluent Inc., Fluent User's Guide 16.0, 2015.

[8] Menter F R, "Two-equation eddy-viscosity turbulence models for engineering applications", *AIAA J*, **Vol. 32**, pp. 1598–1605, 1993.

[9] Hirt C W, Nichols B D, "Volume of fluid method for the dynamics of free boundaries", *Journal of Computational Physics*, **Vol. 39**, pp. 201–225, 1981.

[10] Egorov Y, "Validation of CFD codes with PTS-relevant test cases",EVOL-ECORA-D07, 2004.

[11] *Final Publishable JRP Report Multiphase flow metrology in oil and gas production (ENG58),* Euramet, 2018.

[12] Fiebach A, Schmeyer E, Knotek S, Schmelter S, "Numerical simulation of multiphase flow in a vertically mounted Venturi flow meter", in: *Proceedings of FLOMEKO*, 2016.

[13] Olbrich M, Schmeyer E, Riazy L, Oberleithner K, Bär M, Schmelter S. "Validation of simulations in multiphase flow metrology by comparison with experimental video observations", *IOP Conf. Series: Journal of Physics: Conf. Series*, **Vol. 1065**, 2018.

[14] Taitel Y, Barnea D, "A consistent approach for calculating pressure drop in inclined slug flow", *Chem. Eng. Sci.*, **Vol. 45**, pp. 1199-1206, 1990.

[15] Al-Kayiem H H, Mohmmed A O, Al-Hashimy Z I, Time R W, "Statistical assessment of experimental observation on the slug body length and slug translational velocity in a horizontal pipe", *International Journal of Heat and Mass Transfer*, **Vol. 105**, pp. 252-260, 2017.

[16] Baba Y D, Aliyu A M, Archibong A E, Abdulkadir M, Lao L, Yeung H, "Slug length for high viscosity oil-gas flow in horizontal pipes: Experiments and prediction", *Journal of Petroleum Science and Engineering,* **Vol. 165**, pp. 397-411, 2018.

[17] Brossard C, Monnier J-C, Barricau P, Vandernoot F-X, Le Sant Y, Champagnat F, Le Besnerais G, "Principles and Applications of Particle Image Velocimetry", *AerospaceLab Journal,* 2009.